Interaction of acridine-calix[4]arene with DNA at the electrified liquid|liquid interface

Francine Kivlehan,[a] Myriam Lefoix,[b] Humphrey A. Moynihan,[b] Damien Thompson,[a] Vladimir I. Ogurtsov,[a] Grégoire Herzog,[a] Damien W. M. Arrigan,[a,1,2,*]

[a] Tyndall National Institute, Lee Maltings, University College Cork, Cork, Ireland.

[b] Department of Chemistry, Analytical and Biological Chemistry Research Facility, University College Cork, Cork, Ireland.

[1] ISE Member.

[2] Current address: Nanochemistry Research Institute, Department of Chemistry, Curtin University of Technology, GPO Box U1987, Perth, WA 6845, Australia.

* Author for correspondence: Email : d.arrigan@curtin.edu.au; fax: +61-(0)8-9266----; phone +61-(0)8-9266-9735.

Abstract

The behaviour of an acridine-functionalized calix[4]arene at the interface between two immiscible electrolyte solutions (ITIES) is reported. Molecular modelling showed that the acridine-calix[4]arene has regions of significant net positive charge spread throughout the protonated acridine moieties, consistent with it being able to function as an anion ionophore. The presence of this compound in the organic phase facilitated the transfer of aqueous phase electrolyte ions. Upon addition of double stranded DNA to the aqueous phase, the transfer of electrolyte anions was diminished, due to DNA binding to the acridine moiety at the ITIES. The behaviour provides a basis for DNA hybridization detection using electrochemistry at the ITIES.

Keywords: calixarene, acridine, DNA, voltammetry, impedance, interface, ITIES.

1. Introduction.

Electrochemistry at the liquid | liquid interface, or at the interface between two immiscible electrolyte solutions (ITIES), [1,2] has been developed as an electroanalytical strategy for the detection of a variety of biological molecules including amino acids, peptides, proteins, drugs, carbohydrates, neurotransmitters and DNA [3-7]. The use of the ITIES to study cation binding to DNA has been reported [5], whereby binding of DNA to the cation of interest in the aqueous phase resulted in a decrease of transfer current. The voltammetric behaviour of DNA at a polarized liquid|liquid interface in the presence of a cationic surfactant [6] showed that adsorption of DNA at the interface facilitated the transfer of the surfactant from the organic to the aqueous phase. A similar effect was also reported for DNA-cation binding [5]. Furthermore, label-free detection of DNA hybridization on a supported liquid|liquid interface has been reported [7]. Although there is wide interest in the use of electrochemical methods for the study and detection of DNA hybridization at solid electrodes [8], the use of electrochemistry at the ITIES has hardly been addressed [7]. Furthermore, the electrochemistry at the ITIES may be a useful tool for understanding of DNA binding to small molecules [6].

Acridine and its derivatives are a well-established class of DNA and RNA binding agents [9]. These compounds feature a planar chromophore moiety capable of binding reversibly to DNA by intercalation. DNA intercalators undergo non-covalent binding to DNA by insertion between the adjacent base pairs of the double helix [10,11]. In fact, the concept of intercalation was first introduced to explain the reversible and non-covalent binding interactions between acridines and DNA. Calixarenes are a family of synthetic macrocyclic receptors which can be functionalised to provide selectivity toward targeted species. They have been extensively used in electroanalysis [12] although their use as platforms for DNA interaction reagents has not been reported.

We report here the synthesis of an acridine-functionalised calix[4]arene (5,11,17,23-tetra-p-tert-butyl-25,27-bis[[4-acridinyl)butyl]-oxy]-26,28-dipropyl-calix[4]arene, Figure 1) and its

interaction by intercalation with DNA molecules at the polarised water | 1,2-dichloroethane (1,2DCE) interface. We investigated the interactions at the ITIES by cyclic voltammetry (CV) and electrochemical impedance spectroscopy (EIS) as well as study of the possibilities for ion-binding by this compound using molecular modelling. Interactions between DNA and such acridine-calix[4]arene compounds may provide a basis for DNA hybridization detection, based on the concept that the acridine-calix[4]arene may self-assemble at the ITIES to have its acridine moieties protruding into the aqueous phase, where they are available for intercalation with double stranded DNA (dsDNA). This interaction should modulate the electrochemical behaviour of the ITIES.

2. Experimental

2.1. Reagents

All reagents were purchased from SigmaAldrich Ireland (Dublin, Ireland). Aqueous solutions were prepared in ultrapure water ($\geq$ 18 MΩ cm resistivity) from an Elgastat Maxima-HPLC water purification unit (Elga, UK). dsDNA samples were prepared from sodium salts of calf thymus DNA (SigmaAldrich). Each strand was 214 base pairs in length, with a molecular weight of 139,100 g mol^{-1}. Solutions were prepared in ultrapure water and concentrations determined by spectrophotometry at 260 nm, yielding sample concentrations of 1.36 x 10^{-7} M. These were aliquoted into 10 μL volumes and stored frozen until required. The acridine-calix[4]arene compound was synthesised as described below. Solvents used in the synthesis were distilled and dried using standard general methods. Silica gel 60 (0.035-0.070 mm, 220-440 mesh) was obtained from Fluka.

2.2. Compound characterisation.

Melting points were determined using an Electrothermal 9100 melting point apparatus and are uncorrected. ^{1}H NMR and ^{13}C NMR spectra were recorded with a Bruker Avance 300 (300 MHz)

spectrometer in $CDCl_3$ with Me_4Si employed as an internal standard. Infrared (IR) spectra were recorded on a Perkin-Elmer 1000 spectrometer. Mass spectrometric analysis was performed with a Waters Micromass Quattro micro mass spectrometer, using electrospray ionisation (ES+). The presence of solvent in the samples was confirmed by ^{1}H NMR spectroscopy.

2.3. Synthesis of the acridine-calix[4]arene compound.

The di-amino calix[4]arene compound, 5,11,17,23-tetra-*p*-tert-butyl-25,27-bis[(aminobutyl)oxy]-26,28-dipropoxycalix[4]arene, was first prepared based on the reported procedure of Scheerder *et al.* [13]. Spectroscopic data were in good agreement with the literature values [13].

9-chloroacridine was prepared in 2 steps. First, 2-(phenylamino)benzoic acid was prepared. A mixture of aniline (7.6 mL, 83.4 mmol, 6.37 eq), *o*-chlorobenzoic acid (2.05 g, 13.10 mmol, 1 eq), sodium carbonate (2.05 g, 14.8 mmol, 1.12 eq) and copper in powdered form (0.5 g, 7.87 mmol, 0.6 eq) was heated at reflux for 2 hours. After cooling to room temperature, a 1:1 v/v mixture of concentrated HCl/water (12 mL/12 mL) was added. After vigorous shaking, the precipitate was filtrated and dissolved in 4.0 M sodium hydroxide. Charcoal was then added to the solution, boiled for 2 minutes and filtered over celite whilst hot. The filtrate was then acidified with concentrated HCl and the resulting precipitate filtrated and dried in the oven at 60 °C to afford a beige solid: 1.39 g, yield 50%, melting point 182 – 184 °C (literature value 187 – 188 °C [14]). ^{1}H NMR: 6.76 (t, 1H, C**H** ar, ^3J = 8.0 Hz), 7.14 (t, 1H, C**H** ar, ^3J = 7.2 Hz), 7.21-7.40 (m, 6H, C**H** ar), 8.05 (dd, 1H, C**H** ar, ^3J = 8.0 Hz, ^4J = 1.5 Hz), 9.31 (sl, 1H, N**H**), 11.88 (COO**H**). ^{13}C NMR: 114.2 (CH ar), 117.3 (CH ar), 123.3 (2 CH ar), 124.2 (CH ar), 129.6 (2 CH ar), 132.8 (CH ar), 135.4 (CH ar), 140.5 (2 Cq), 149.1 (Cq), 173.9 (C=O). IR (KBr): 745, 891, 1266, 1438, 1510, 1577, 1599, 1658. MS (ES+): *m/z* = 214 $[M-H]^+$. MS (ES -): *m/z* = 212 $[M-H]^-$.

Second, 9-chloroacridine was prepared as a mixture of 2-(phenylamino)benzoic acid (500 mg, 2.34 mmol, 1 eq), phosphorusoxychloride (983 µL, 10.55 mmol, 4.5 eq) and sulfuric acid (5 µL, 0.09 mmol, 0.04 eq), which was heated at reflux for 11 hours. After cooling to room

temperature the solution was slowly added to cracked ice (60 g) and made slightly alkaline with aqueous ammonia (33%). The precipitate obtained was filtrated, washed with water and air-dried over 24 hours. The residue obtained was purified by chromatography (eluent THF/hexane/Et_3N (20:75:5 v/v/v)) to give a yellow solid: 340 mg, yield 68%, melting point 121 – 123 °C (literature value 122 °C [15]). ^{1}H NMR: 7.65 (td, 2H, C**H** ar, ^3J = 7.8 Hz, ^4J = 1.2 Hz), 7.83 (td, 2H, C**H** ar, ^3J =7.8 Hz, ^4J = 1.2 Hz), 8.24 (d, 2H, C**H** ar, ^3J = 7.8 Hz), 8.45 (d, 2H, C**H** ar, ^3J = 7.8 Hz). ^{13}C NMR: 124.3 (Cq), 124.7 (CH ar), 127.0 (CH ar), 129.7 (CH ar), 130.7 (CH ar), 141.4 (Cq), 148.8 (Cq). IR (KBr): 942, 1145, 1391, 1512. MS (ES +): *m/z* = 214 $[MH]^+$ with ^{35}Cl, *m/z* = 216 $[MH]^+$ with ^{37}Cl.

The bifunctional acridine-calix[4]arene compound was prepared by substitution of the di-amino calix[4]arene with 9-chloroacridine. Synthesis was performed based on a reaction pathway previously reported [16]. A mixture of 5,11,17,23-tetra-*p*-tert-butyl-25,27-bis[(aminobutyl)oxy]-26,28-dipropoxycalix[4]arene (2 g, 2.28 mmol), phenol (19 g, 201.89 mmol) and 9-chloroacridine (1.95 g, 9.12 mmol) was stirred for 19 hours at 85 – 90 ºC. The phenol was eliminated by sublimation and the residue obtained was purified by chromatography (eluent hexane/ethlyacetate (8:2 v/v), ethlyacetate then ethlyacetate/methanol (8:2 v/v)) to give a yellow solid: 1.34 g, yield 48%, melting point 193 – 195 °C. ^{1}H NMR: 0.83 (s, 18H, C(C**H$_3$**)$_3$), 0.98 (t, 6H, $OCH_2CH_2C\mathbf{H_3}$, ^3J= 7.3 Hz), 1.35 (s, 18H, C(C**H$_3$**)$_3$, 1.87-1.97 (m, 4H, $OCH_2C\mathbf{H_2}CH_3$), 2.21-2.27 (m, 4H, $OCH_2CH_2C\mathbf{H_2}CH_2NH$), 2.27-2.43 (m, 4H, $OCH_2C\mathbf{H_2}CH_2CH_2NH$), 3.16 (d, 4H, ArC**H**HAr), *J*= 12.4 Hz), 3.65 (t, 4H, $OC\mathbf{H_2}CH_2CH_3$, *J*= 7.2 Hz), 4.18-4.26 (m, 8H, $OC\mathbf{H_2}CH_2CH_2C\mathbf{H_2}NH$), 4.41 (d, 4H, ArCH**H**Ar, *J*= 12.4 Hz), 6.46 (s, 4H, C**H** calix), 7.13 (s, 4H, C**H** calix), 7.25 (t, 4H, C**H** acrid, *J*= 7.7 Hz), 7.49 (t, 4H, C**H** acrid, *J*= 7.7 Hz), 8.04 (d, 4H, C**H** acrid, *J*=7.7 Hz), 8.56-8.60 (m, 4H, C**H** acrid), 10.46 (bs, 2H, N**H**). ^{13}C NMR: 11.0 (2 $OCH_2CH_2\mathbf{C}H_3$), 23.9 (2 $OCH_2\mathbf{C}H_2CH_3$), 26.7 (2 $OCH_2CH_2\mathbf{C}H_2CH_2NH$), 27,8 (2 $OCH_2\mathbf{C}H_2CH_2CH_2NH$), 31.3 (2 C(**C**H$_3$)$_3$), 31.3 (4 CH_2Ar), 31.9 (2 C(**C**H$_3$)$_3$), 33.7 (2 **C**(CH$_3$)$_3$), 34.2 (2 **C**(CH$_3$)$_3$), 49.3 ($2OCH_2CH_2CH_2\mathbf{C}H_2NH$), 74.2 (2 $O\mathbf{C}H_2CH_2CH_2CH_2NH$), 77.7 (2

O**C**$H_2CH_2CH_3$), 112.5 (2 **Cq**), 119.6 (4 **C**H acrid), 123.2 (4 **C**H acrid), 124.6 (4 **C**H calix), 125.6 (4 **C**H acrid), 125.7 (4 **C**H calix), 125.7 (2 **Cq**), 131.8 (4 **Cq**), 134.0 (4 **C**H acrid), 135.7 (6 **Cq**), 140.2 (2 **Cq**), 144.2 (2 **Cq**), 145.2 (2 **Cq**), 152.6 (2 **Cq**), 154.6 (2 **Cq**), 157.0 (2 **Cq**). IR (KBr): 1197, 1480, 1589, 1636, 2960. MS (ES +): *m/z* = 1231 $[MH]^+$, 1053 [M-acridine]$^+$, 616 $[M/2+H]^+$.

2.4. Electrochemical measurements

Electrochemical measurements were recorded using CHI660B (CH Instruments, Austin, Texas), or Autolab PGSTAT30 (EcoChemie BV, Utrecht, The Netherlands) potentiostats. The electrochemical cell used was:

Ag | AgCl | 10 mM BTPPACl, 10 mM LiCl | 10 mM BTPPATPClB (1,2-DCE) || aqueous phase | Ag_nX_m | Ag

and was operated in four electrode mode, with platinum mesh counter electrodes in each phase, a Ag|AgCl electrode for the organic phase and either a Ag|AgCl or Ag|Ag_3PO_4 electrode for the aqueous phase, depending on the aqueous phase electrolyte. The organic phase electrolyte, bis-(triphenylphosphoranylidene)ammonium tetrakis(4-chlorophenylborate) (BTPPATPClB), was prepared by metathesis of potassium tetrakis(4-chlorophenyl)borate (KTPClB) and bis(triphenylphosphoranylidene) ammonium chloride (BTPPACl). Additions of the acridine-calix[4]arene were made to the organic phase using a glass microlitre syringe (Carl Stuart Ltd., Switzerland). The ITIES was flat in appearance and had a geometric area of 0.78 cm^2.

2.5. Molecular modelling.

Calix[4]arene models were generated from the experimental nuclear coordinates of the neutral tetraethyl-p-tert-butyl calix[4]arene tetraacetate structure [17]. Force field parameters for the parent methoxy-p-tert-butylcalix[4]arene host were taken from published data [18] and acridine derivatives were created by replacing the methoxy groups with two propoxy and two neutral/protonated acridine groups, and described using existing parameters [19]. Each model

was solvated in a simulation cell of standard TIP3P water molecules of edge length 4.0 nm, and periodic boundary conditions applied. Five nanoseconds of molecular dynamics were performed for each host at constant room temperature and pressure with a Nose–Hoover algorithm, following minimisation and 300 picoseconds of thermalisation with gradually reducing constraints on the host heavy atoms. Bonds involving hydrogen were constrained to their experimental lengths with the SHAKE algorithm. The CHARMM program [20] version c31b2 was used for all molecular dynamics (MD) simulations. The electronic properties of the final MD structures, stripped of solvent, were obtained using Gaussian03 software (Gaussian, Inc., www.gaussian.com) with the B3LYP functional [21] and 6-31G* basis sets. Stable geometries were obtained via nuclear relaxation, followed by electronic structure determination using the gfoldprint and POP=FULL keywords to generate output files formatted for molecular electrostatic potential visualisation using MOLEKEL (Molecular Visualisation Software, University of Geneva, www.bioinformatics.org/molekel/wiki/).

3. Results and Discussion

3.1. Synthesis and characterisation.

The required acridine-calix[4]arene was prepared from a known bis(aminobutyl)-functionalised calix[4]arene [13] by reaction with freshly prepared 9-chloroacridine. This was produced in gram quantities as a yellow crystalline solid which was characterised by ^{1}H and ^{13}C NMR spectroscopy and mass spectrometry. It was easily prepared as a solution in 1,2DCE, the organic solvent employed in electrochemical studies at the ITIES.

3.2. Molecular modelling.

Molecular modelling studies were employed to show the distribution of charge over the surface of the molecules as a function of pH and to show that the pH of the aqueous phase has a strong influence on the interactions between the two acridine moieties. At pH values below acridine's

pKa the nitrogen groups are protonated, while above it, the lone pairs on the nitrogen groups are unaffected. Although the pKa of acridine is 5.6 [22], 9-aminoacridine is a stronger base. The pKa of 9-aminoacridine is 9.9 [23]. In the neutral form (pH > pKa), there are significant zones of net negative charge on the the alkoxy oxygens and acridine ring nitrogens (Fig. 2(A)) which may serve as binding sites for cations [17]. When the acridine moieties are protonated (Fig. 2(B)), there are significant zones of net positive charge present on the acridine tail (formal charge of 2+). The blue areas carry a higher level of surface charge activity compared to the calix[4]arene ring section, which is depicted as the green area in Figure 2. These results also provide a strong indication that the protonated acridine-calix[4]arene may serve as an ionophore for anions [24,25] when present in the organic phase. Regions of net negative charge also exist on the oxygen groups of the alkyl chains that may serve as binding sites for cations, but these are less intense than the areas of positive charge on the protonated acridine moieties.

The possibility of π-π interactions between the two acridine moieties resulting in π-stacking in the neutral acridine state was also considered. The results show that a high population of stacked conformations can exist for the acridine-calix[4]arene when the acridine moieties are uncharged (Fig. 2(C)). In the protonated form, however, proton-proton repulsion decreases π-π stacking due to significant zones of positive charge present on the acridine tail. Anionic species binding between the acridine groups may reduce this repulsion and create a more ordered, neutral-type, tail, though this was not explicitly modelled in the present work.

3.3. Cyclic Voltammetry.

CV in the absence and in the presence of organic-phase acridine-calix[4]arene was undertaken with a variety of aqueous electrolyte solutions. Under acidic aqueous phase conditions, the CVs exhibited “electrochemical instabilities” [26,27] associated with ion transfer reactions when the acridine-calix[4]arene was present in the organic phase (Figure 3). When 0.1 M HCl was used as the aqueous phase, large electrochemical instabilities [26,27] were obtained during CV

following the addition of the acridine-calix[4]arene to the organic phase. A similar response was also seen when 0.1 M LiCl was used as the aqueous phase electrolyte (Figure 3). This instability was present despite stable background voltammograms recorded prior to addition of the acridine-calix[4]arene to the cell. The instability is thus attributed to the presence of the acridine-calix[4]arene. The pH of aqueous 0.1 M LiCl was ca. pH 5, so that both aqueous phases presented in Figure 3 were sufficiently acidic to protonate the acridine moiety (the pKa of the acridine moiety is 9.9 [23]). The instability is consistent with the location of the acridine-calix[4]arene compound at the ITIES such that the polar hydrophilic protonated acridine tail is localised at the interface and protruding into the aqueous phase, while the hydrophobic calix[4]arene macrocycle is located in the organic phase. The interfacial localisation of calixarene derivatives, such as at the water-chloroform interface, is well known from computational studies [28,29], where is has been shown they orientate at the interface according to hydrophobic/hydrophilic interactions. The electrochemical instabilities presented in Figure 3 provide experimental verification of such localisation for the acridine-calix[4]arene molecule studied here.

However at neutral pH, such instabilities were not evident (Figure 4), although the acridine moieties may be expected to be protonated if they protrude into the aqueous phase. Nevertheless, depending on the aqueous phase electrolyte, the presence of acridine-calix[4]arene in the organic phase resulted in the appearance of one or two pairs of reversible ion transfer peaks (Figure 4; Table 1). The results from a range of aqueous electrolytes were similar, with two sets of transfer peaks observed for NaH_2PO_4, PBS and SSC buffer solutions upon addition of the acridine-calix[4]arene to the organic phase. The peak currents for both ion transfer processes were linear with the square root of the voltammetric scan rate, indicating a diffusion-controlled ion transfer process. Furthermore, the peak-to-peak potential separations, ΔE_p, were close to the theoretical 59 mV expected for transfer of an ion carrying a single (positive or negative) charge. Thus, by use of the Randles-Sevcik equation (1)

$$I_p = 2.81x10^5 z_i^{3/2} AC_i D^{1/2} \upsilon^{1/2} \quad (1)$$

(where z_i is the charge of the transferring ion, C_i the concentration, D the diffusion coefficient and v the potential sweep rate) the diffusion coefficient associated with the ion transfer process (assuming a charge of 1) was calculated from the experimental data. Due to the experimental conditions (where the aqueous phase electrolyte concentration was in excess over the organic phase acridine-calix[4]arene concentration) the ion transfer peak currents were limited by the diffusion of acridine-calix[4]arene in the organic phase. The diffusion coefficients in Table 1 refer, therefore, to the diffusion of the acridine-calix[4]arene compound to the ITIES, whereas the charge transfer process may be due to facilitated transfer of anion species from the aqueous phase electrolytes by protonated acridine-calix[4]arene. Given the nature of the acridine-calix[4]arene compound, as discussed above in the molecular modelling section, it is suggested that the transfer peaks observed (Figure 4) are due to the facilitated transfer of anion species from the aqueous phase to the organic phase, with the obvious candidates being the chloride and phosphate anions present in most of the electrolyte solutions examined. The presence of two pairs of peaks in the CVs may thus be attributed to transfers of chloride and a phosphate species at different potentials or to transfers of two phosphate species (i.e. $H_2PO_4^-$ and HPO_4^{2-}) at different potentials, facilitated by interaction with the acridine-calix[4]arene.

Upon addition of the dsDNA to the aqueous phase, the CV peaks were diminished (Figure 4A). The peak heights were further decreased on prolonging of the reaction time after addition of dsDNA. The decrease of the peak currents (Figure 4A) upon addition of dsDNA to the aqueous phase when the organic phase contained the acridine-calix[4]arene compound is attributed to the intercalative interactions of dsDNA with the acridine moeities located at the interface. This interaction, in turn, lowers the number of acridine-calix[4]arene sites available at the ITIES for facilitated transfer of aqueous phase electrolyte anions as well as inhibition of the facilitated transfer that may occur with acridine-calix[4arene molecules that remain at the interface but are unbound to dsDNA.

Control experiments on the behaviour of dsDNA at the ITIES in the absence of organic phase acridine-calix[4]arene did not reveal any ion transfer peak currents (data not shown). In such an experiment, addition of dsDNA to the PBS (pH ~ 7.4) aqueous phase did not result in any ion-transfer reactions, in contrast to the ion transfer that occurred upon addition of the acridine-calix[4]arene to the cell. Control experiments on the behaviour of the ITIES containing organic phase acridine-calix[4]arene but without added dsDNA in the aqueous phase (Fig. 4B), did not show any change in the ion transfer peak currents over the same timescale as used in Fig. 4A. These control experiments indicate that the DNA-acridine intercalation process causes the change in the CV curves shown in Fig. 4A.

3.4. Electrochemical Impedance Spectroscopy.

Interactions between the acridine-calix[4]arene and dsDNA were studied by EIS at the ITIES. Impedance spectra in the frequency (*f*) range 0.118 Hz – 9615 Hz at an applied potential of 0.45 V and an ac amplitude of 50 mV were recorded for the ITIES cell in the absence and presence of 0.321 mM acridine-calix[4]arene (organic phase) and after addition of 0.68 nM dsDNA (aqueous phase). The ac amplitude was chosen based on experimental variation of the value; 50 mV provided us with the most reproducible data and enabled a qualitative study of DNA binding with the acridine-calix[4]arene compound at the ITIES. Figure 5 shows Nyquist plots (imaginary part of the impedance (Z(im)) versus the real part of the impedance (Z(re)). Figure 6 shows the Bode plots (dependence of both Z(im) and Z(re) on the frequency *f*). These plots are presented in double logarithmic scale because of the large changes in impedance over the frequency range investigated.

The frequency spectra indicate that addition of the acridine-calix[4]arene compound to the cell significantly changes behaviour. The result of the addition is a dramatic (ca. one order of magnitude) drop of the impedance values and the modification of the impedance spectra. The

variations due to acridine-calix[4]arene addition include a decrease of the slope in the Bode plots (Figure 6) and the disappearance of the upright portion of the spectra in the Nyquist plots (Figure 5). These modifications occur mainly at low frequencies (< 10 Hz), where system behaviour is defined mostly by diffusion processes. Parameters extracted from the impedance data provide information on the physical nature of the processes occurring at the ITIES as well as indicating parameters which may be used in a dsDNA detection method. In this case, analysis of the interfacial capacitance, obtained using equation (2),

$$Cs(f_k) = -\frac{1}{[Z(im)(f_k)]2\pi f} \qquad (2)$$

(where $Z(im)(f_k)$ is the imaginary part of the complex impedance at the specified frequency f_k) showed that it was independent of frequency in the range up to 100 Hz in the absence of acridine-calix[4]arene and dsDNA (Figure 7). But addition of acridine-calix[4]arene to the organic phase resulted in a change to the $1/\sqrt{f}$ dependence of the capacitance (Figure 7), due to the occurrence of diffusion-controlled facilitated transfer of aqueous phase electrolyte ions, as also seen by CV (Fig. 4).

The impedance dependencies also revealed the occurrence of binding of dsDNA to acridine-calix[4]arene moieties at the ITIES. This follows from Figure 8, which presents the frequency dependence of relative difference between the capacitances in the presence of organic phase acridine-calix[4]arene and the absence and presence of dsDNA in the aqueous phase, $\delta Cs=(Cs_{calix}-Cs_{dsDNA})/Cs_{calix}$. Here, Cs_{calix} refers to the capacitance in the presence of organic phase acridine-calix[4]arene but without aqueous phase dsDNA, whereas Cs_{dsDNA} refers to the capacitance in the presence of both organic phase acridine-calix[4]arene and aqueous phase dsDNA. It can be seen that the DNA – acridine-calix[4]arene binding event can be clearly detected in the frequency range between 0.1 Hz and 100 Hz, with an average relative

differential signal of ca. +4.4 % for *Cs*. These relative changes of the capacitance from the impedance signal due to DNA – acridine-calix[4]arene binding at the ITIES binding coincide with the values reported for the solid electrode-based impedimetric DNA sensors [28].

4. Conclusions.

The electrochemical behaviour of a bifunctional acridine-calix[4]arene compound has been investigated using liquid|liquid electrochemistry. A range of aqueous electrolytes were employed during the course of this study, with acridine-calix[4]arene present in the organic phase. CV results show that this compound readily behaves as an ionophore for ions present in the aqueous phase, yielding a range of ion-transfer reactions. While earlier molecular modelling studies [28,29] showed that calix[4]arene derivatives align at the liquid/liquid interface according to hydrophilic/hydrophobic interactions, in the present work, modelling revealed that the acridine-calix[4]arene compound exhibits zones of net positive charge spread throughout the acridine moieties at physiological pH, providing a strong indication that this compound can function as an ionophore for anions when present in the organic phase. The most likely candidates for assisted ion-transfer reactions taking place are chloride and phosphate, as these were present in all or most of the aqueous electrolytes examined. These transfer currents were decreased upon addition of dsDNA to the aqueous phase, due to acridine-calix[4]arene-induced adsorption of dsDNA at the liquid|liquid interface. This is induced by the highly-favoured intercalative binding of the acridine moieties with dsDNA. EIS experiments support this scenario, with small changes in impedance or capacitance being recorded. Although the relative signal changes obtained by CV and EIS are ca. 40 % and 4 %, respectively, the methods are in qualitative agreement that a change in electrochemical property of the cell occurs on binding of the dsDNA to the acridine-calix[4]arene. The study of this new acridine-calix[4]arene compound has revealed that it has DNA binding properties at the ITIES, based on the acridine functionality. In due course it may be used as the basis for DNA hybridisation detection.

Acknowledgements.

This work was performed with the support of Science Foundation Ireland (SFI) (grants 02/IN.1/B84 and 07/IN.1/B967) and the Irish Research Council for Science, Engineering and Technology (grants RS/2004/74 (FK) and PD/2005/23 (GH)). Molecular modelling was performed at Tyndall National Institute using computer resources provided by SFI and at the SFI/Higher Education Authority Irish Centre for High-End Computing (ICHEC). Discussions with Dr. J. Strutwolf and Dr. P. Galvin are gratefully acknowledged.

References.

[1] Z. Samec, Pure Appl. Chem., 76 (2004) 2147.

[2] R.A.W. Dryfe, Adv. Chem. Phys., 141 (2009) 153.

[3] G. Herzog, D.W.M. Arrigan, Analyst, 132 (2007) 615.

[4] D.W.M. Arrigan, Anal. Lett., 41 (2008) 3233.

[5] B.R. Horrocks, M.V. Mirkin, Anal. Chem., 70 (1998) 4653.

[6] T. Osakai, H. Komatsu, M. Goto, J. Phys.: Condens. Matter, 19 (2007) 375103.

[7] M.Y. Vagin, S.A. Trashin, A.A. Karyakin, M. Mascini, Anal. Chem., 80 (2008) 1336.

[8] K.J. Odenthal, J.J. Gooding, Analyst, 132 (2007) 603.

[9] W.A. Denny, Curr. Med. Chem., 9 (2002) 1655.

[10] A. Kamal, O. Srinivas, P. Ramulu, G. Ramesh, P.P. Kumar, Bioorg. Med. Chem. Lett., 14 (2004) 4107.

[11] L.S. Lerman, J. Mol. Biol., 3 (1961) 18.

[12] K.M. O'Connor, D.W.M. Arrigan, G. Svehla, Electroanalysis, 7 (1995) 205.

[13] J. Scheerder, M. Fochi, J.F.F. Engbersen, D.N. Reinhoudt, J. Org. Chem., 59 (1994) 7815.

[14] R. Carrasco, R.F. Pellon, J. Elguero, P. Goya, J.A. Paez, Synth. Commun. 19 (1989) 2077.

[15] S. Skonieczny, Heterocycles, 9 (1978) 1335.

[16] G.D. Jaycox, G.W. Gribble, M.P. Hacker, J. Heterocycl. Chem., 24 (1987) 1405.

[17] J. Wickens, R.A.W. Dryfe, F.S. Mair, R.G. Pritchard, R. Hayes, D.W.M. Arrigan, New J. Chem., 24 (2000) 149.

[18] S. Fischer, P.D.J. Grootenhuis, L.C. Groenen, W.P. van Hoorn, F.C.J.M. van Veggel, D.N. Reinhoudt, M. Karplus, J. Am. Chem. Soc., 117 (1995) 1611.

[19] A.D. MacKerrell, Jr., D. Bashford, M. Bellott, R.L. Dunbrack, Jr., J.D. Evanseck, M.J. Field, S. Fischer, J. Gao, H. Guo, S. Ha, D. Joseph-McCarthy, L. Kuchnir, K. Kuczera, F.T.K. Lau, C. Mattos, S. Michnick, T. Ngo, D.T. Nguyen, B. Prodhom, W.E. Reiher, III, B. Roux, M. Schlenkrich, J.C. Smith, R. Stote, J. Straub, M. Watanabe, J. Wiórkiewicz-Kuczera, D. Yin, M. Karplus, J. Phys. Chem. B, 102 (1998) 3586.

[20] B.R. Brooks, R.E. Bruccoleri, B.D. Olafsen, D.J. States, S. Swaninathan, M. Karplus, J. Comput. Chem., 4 (1983) 187.

[21] A. D. Becke, J. Chem. Phys., 98 (1993) 5648.

[22] S.G. Schulman, A.C. Capomacchia, J. Am. Chem. Soc., 95 (1973) 2763.

[23] C.A. Smith, H.C. Chang, W.S. Stuve, G.J. Atwell, W.A. Denny, J. Phys. Chem., 99 (1995) 8927.

[24] F. Kivlehan, W.J. Mace, H.A. Moynihan, D.W.M. Arrigan, Anal. Chim. Acta, 585 (2007) 154.

[25] F. Kivlehan, W.J. Mace, H.A. Moynihan, D.W.M. Arrigan, Electrochim. Acta, 54 (2009) 1918.

[26] T. Kasahara, N. Nishi, M. Yamamoto, T. Kakiuchi, Langmuir, 20 (2004) 875.

[27] A. Berduque, M.D. Scanlon, C.J. Collins, D.W.M. Arrigan, Langmuir, 23 (2007) 7356.

[28] G. Wipff, E. Engler, P. Guilbaud, M. Lauterbach, L. Troxler, A. Varnek, New J. Chem., 20 (1996) 411.

[29] A. Varnek, G. Wipff, J. Comput. Chem., 17 (1996) 1520.

[30] C. Tlili, H. Korri-Youssoufi, L. Ponsonnet, C. Martelet, N.J. Jaffrezic-Renault, Talanta, 68 (2005) 131.

Figure legends.

Figure 1. Chemical structure of 5,11,17,23-tetra-p-tert-butyl-25,27-bis[[4-acridinyl)butyl]-oxy]-26,28-dipropyl-calix[4]arene, the acridine-calix[4]arene studied in this work.

Figure 2. Computed electrostatic potential surfaces for the acridine-calix[4]arene compound in (A) the neutral non-protonated state and (B) the protonated state. Surfaces were generated from electronic structures as described in the text. Panel (C) plots the relative frequency of occurrence of different inter-ring distances for the acridine tail, averaged over 2500 solvated molecular dynamics structures, as described in the text. The black and grey lines show data for the neutral and protonated species, respectively.

Figure 3. Cyclic voltammetry of the ITIES cell containing different aqueous phase electrolytes. (i) Aqueous = 0.1 M HCl, organic = 10 mM BTPPATPClB + 0.25 mM acridine-calix[4]arene. (ii) Aqueous = 0.1 M LiCl pH ~5, organic = 10 mM BTPPATPClB + 0.21 mM acridine-calix[4]arene. Scan rate: 5 mV s^{-1}. The absence and presence organic phase acridine-calix[4]arene is indicated by (a) and (b), respectively.

Figure 4. (A) Cyclic voltammetry in the absence (_, solid line) and in the presence of 0.214 mM of acridine-calix[4]arene in the organic phase (---, dashed line), 15 minutes after addition of 0.68 nM dsDNA (… , dotted line) and 75 minutes after the addition of 0.68 nM dsDNA (-·-, dash-dot line)to the aqueous phase. Aqueous phase electrolyte: PBS, pH 7.4. Scan rate: 5 mV s^{-1}. (B) as for A, but without addition of dsDNA.

Figure 5. Nyquist plots of the blank electrolyte solutions (■), after addition of 0.321 mM acridine-calix[4]arene (▽) to the organic phase, 20 minutes after addition of 0.68 nM dsDNA (○) to the aqueous phase. Aqueous phase = PBS, pH 7.4, organic phase = 10 mM BTPPATPClB.

Figure 6. Bode plots of the imaginary impedance Z(im) (A) and the real impedance Z(re) (B) as functions of the frequency, for the blank electrolyte solutions (■), after addition of 0.321 mM acridine-calix[4]arene (▽) to the organic phase, and 20 minutes after addition of 0.68 nM dsDNA (○) to the organic phase. Aqueous phase = PBS, pH 7.4, organic phase = 10 mM BTPPATPClB.

Figure 7. Frequency dependencies of the static capacitance of the blank electrolyte solutions (■), after addition of 0.321 mM acridine-calix[4]arene (▽), 20 minutes after addition of 0.68 nM dsDNA (○). Aqueous phase = PBS, pH 7.4, organic phase = 10 mM BTPPATPClB.

Figure 8. Frequency dependence of the relative difference between the static capacitances before and after dsDNA addition. Organic phase contained 0.321 mM acridine-calix[4]arene, aqueous phase contained 0.68 nM dsDNA (after addition). Aqueous phase electrolyte = PBS, pH 7.4, organic phase electrolyte = 10 mM BTPPATPClB.

Table and Figures.

Table 1. Electrochemical parameters obtained from the CV experiments when the acridine-calix[4]arene was present in the organic phase.

Aqueous phase electrolyte	**Acridine-calix[4]arene / mM**	**$E_{1/2}$ / V**	**ΔE_p / V**	**D / $cm^2\ s^{-1}$ (10^{-5})**
10 mM NaCl, pH 7.1	0.27	0.33	0.57	1.13
10 mM NaH_2PO_4, pH 7.0	0.27	0.44	0.60	1.13
		0.58	0.56	1.13
Phosphate buffered saline, pH 7.4	0.27	0.25	0.53	1.13
		0.39	0.62	1.13
Saline sodium citrate, pH 7.0	0.27	0.25	0.64	1.87
		0.39	0.43	1.87

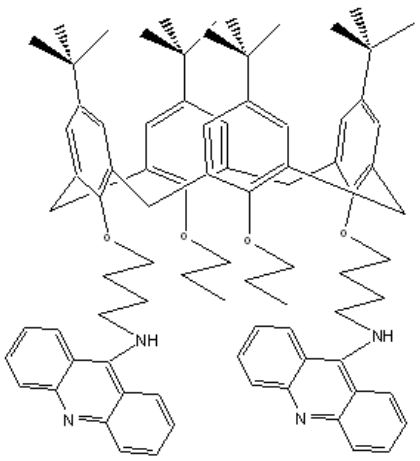

Figure 1. Chemical structure of 5,11,17,23-tetra-p-tert-butyl-25,27-bis[[4-acridinyl)butyl]-oxy]-26,28-dipropyl-calix[4]arene, the acridine-calix[4]arene studied in this work.

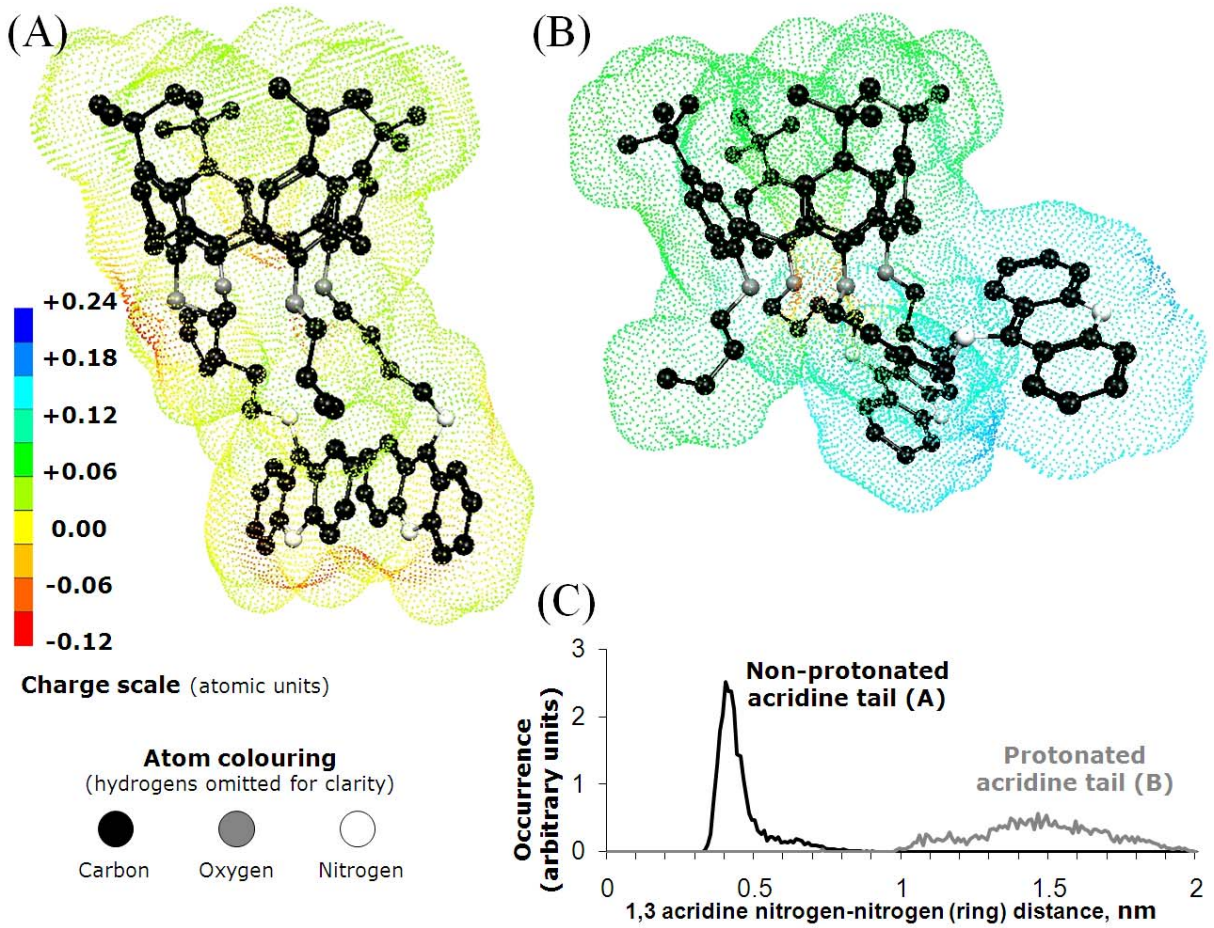

Figure 2. Computed electrostatic potential surfaces for the acridine-calix[4]arene compound in (A) the neutral non-protonated state and (B) the protonated state. Surfaces were generated from electronic structures as described in the text. Panel (C) plots the relative frequency of occurrence of different inter-ring distances for the acridine tail, averaged over 2500 solvated molecular dynamics structures, as described in the text. The black and grey lines show data for the neutral and protonated species, respectively.

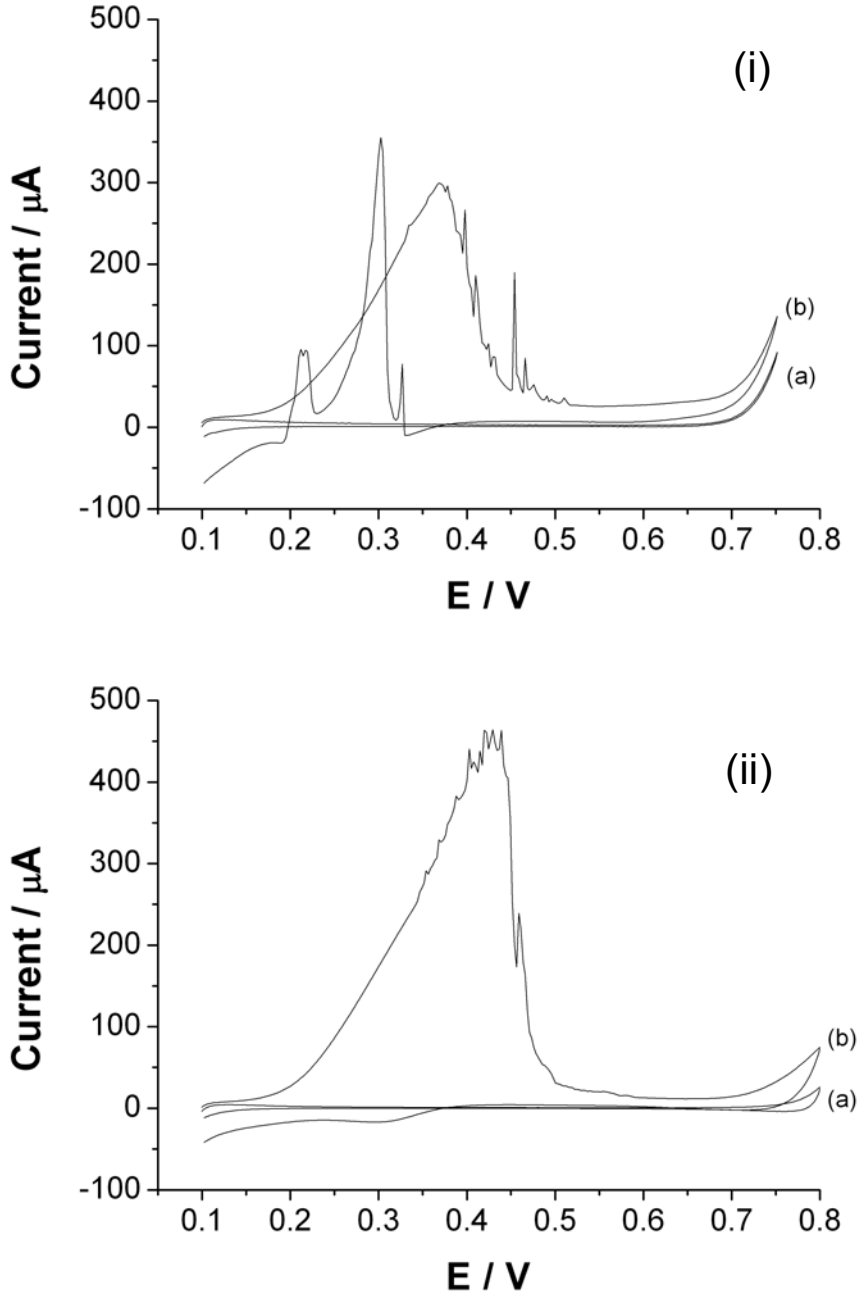

Figure 3. Cyclic voltammetry of the ITIES cell containing different aqueous phase electrolytes. (i) Aqueous = 0.1 M HCl, organic = 10 mM BTPPATPClB + 0.25 mM acridine-calix[4]arene. (ii) Aqueous = 0.1 M LiCl pH ~5, organic = 10 mM BTPPATPClB + 0.21 mM acridine-calix[4]arene. Scan rate: 5 mV s^{-1}. The absence and presence of organic phase acridine-calix[4]arene is indicated by (a) and (b), respectively.

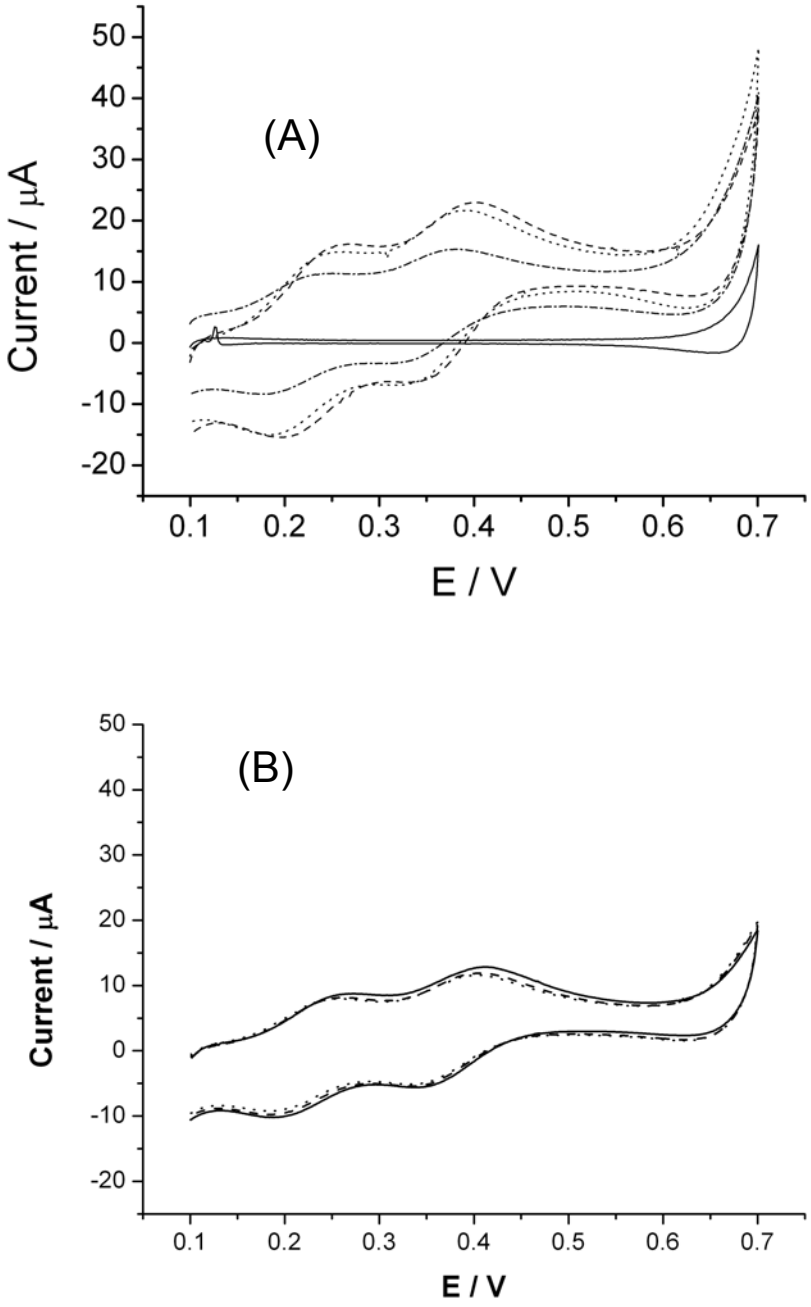

Figure 4. (A) Cyclic voltammetry in the absence (_, solid line) and in the presence of 0.214 mM of acridine-calix[4]arene in the organic phase (---, dashed line), 15 minutes after addition of 0.68 nM dsDNA (… , dotted line) and 75 minutes after the addition of 0.68 nM dsDNA (-·-,

dash-dot line)to the aqueous phase. Aqueous phase electrolyte: PBS, pH 7.4. Scan rate: 5 mV s^{-1}. (B) as for A, but without addition of dsDNA.

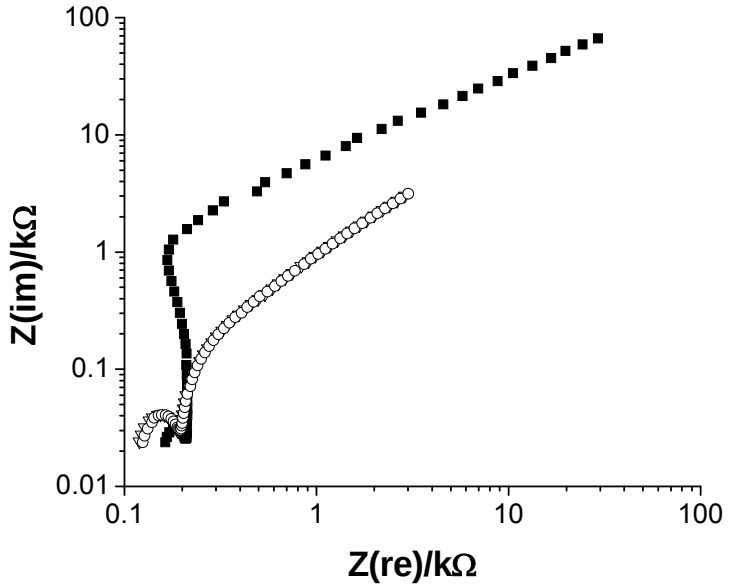

Figure 5. Nyquist plots of the blank electrolyte solutions (■), after addition of 0.321 mM acridine-calix[4]arene (▽) to the organic phase, 20 minutes after addition of 0.68 nM dsDNA (○) to the aqueous phase. Aqueous phase = PBS, pH 7.4, organic phase = 10 mM BTPPATPClB.

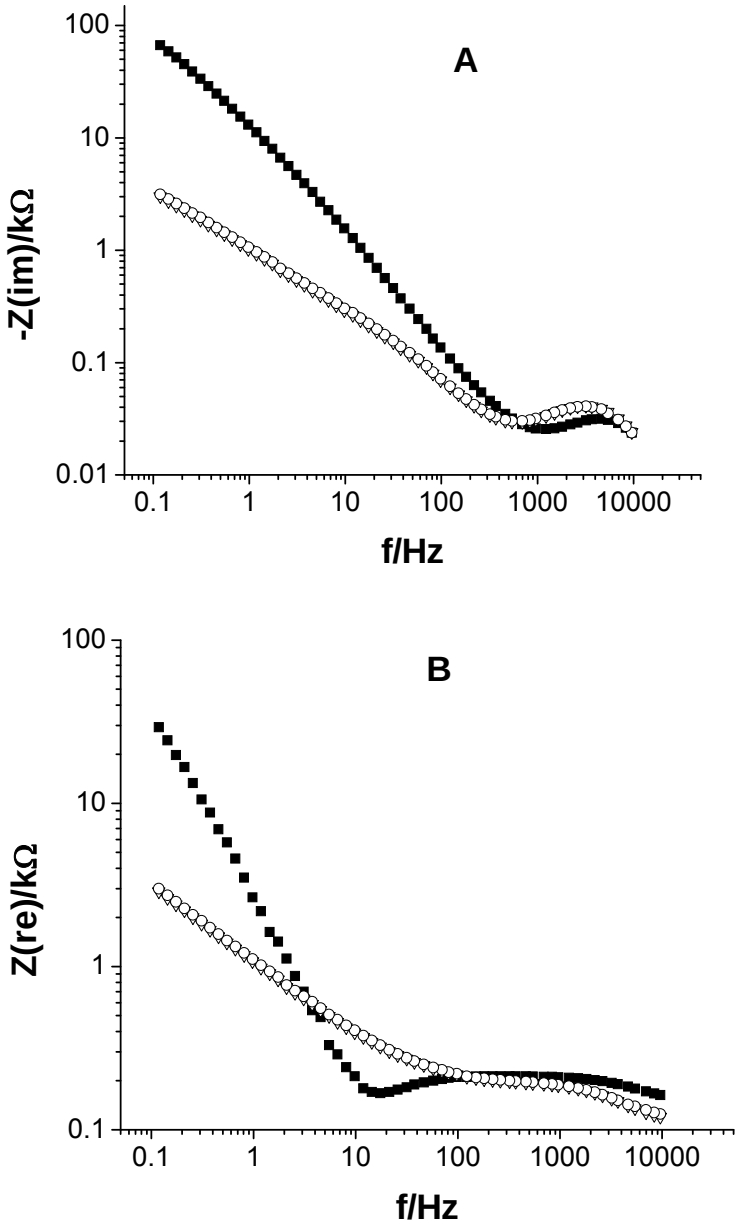

Figure 6. Bode plots of the imaginary impedance Z(im) (A) and the real impedance Z(re) (B) as functions of the frequency, for the blank electrolyte solutions (■), after addition of 0.321 mM acridine-calix[4]arene (▽) to the organic phase, and 20 minutes after addition of 0.68 nM dsDNA (○) to the organic phase. Aqueous phase = PBS, pH 7.4, organic phase = 10 mM BTPPATPCIB.

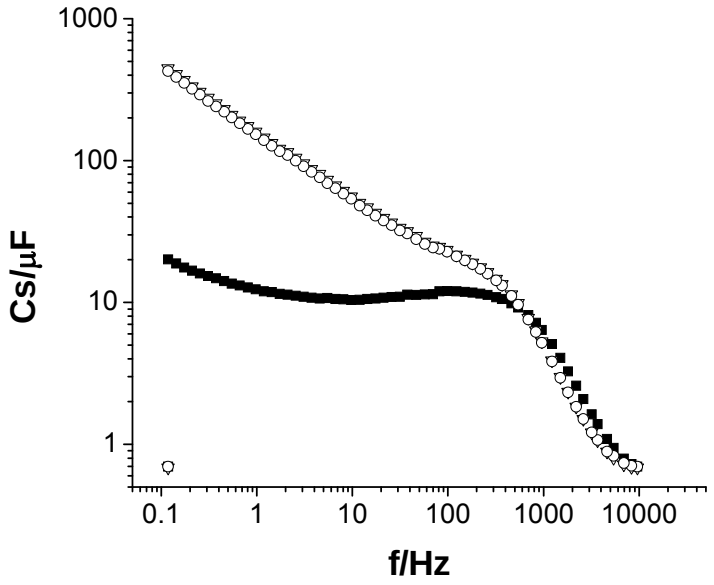

Figure 7. Frequency dependencies of the static capacitance of the blank electrolyte solutions (■), after addition of 0.321 mM acridine-calix[4]arene (▽), 20 minutes after addition of 0.68 nM dsDNA (○). Aqueous phase = PBS, pH 7.4, organic phase = 10 mM BTPPATPClB.

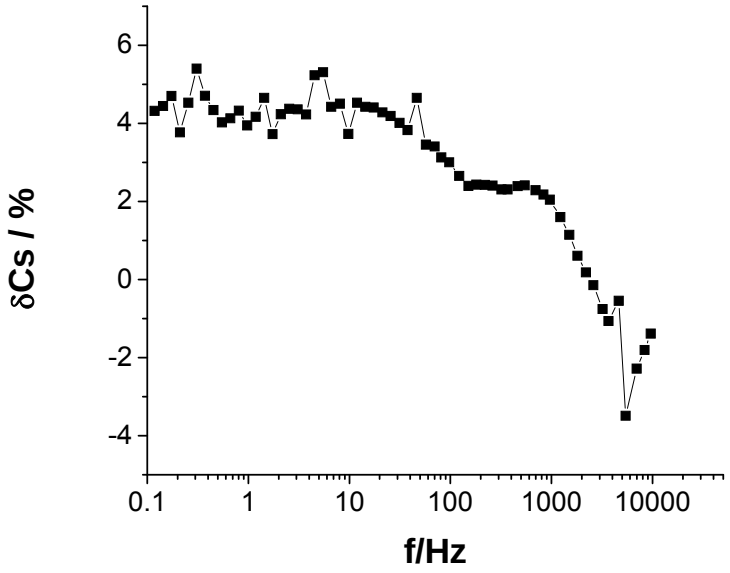

Figure 8. Frequency dependence of the relative difference between the static capacitances before and after dsDNA addition. Organic phase contained 0.321 mM acridine-calix[4]arene, aqueous phase contained 0.68 nM dsDNA (after addition). Aqueous phase electrolyte = PBS, pH 7.4, organic phase electrolyte = 10 mM BTPPATPClB.